Electronic Supplementary Material (ESI) for Nanoscale.

SUPPLEMENTARY INFORMATION

Diameter-dependent thermoelectric figure of merit in single-crystalline Bi nanowires

Jeongmin Kim,[a] Seunghyun Lee,[a] Yuri M. Brovman,[b] Philip Kim,[b] and Wooyoung Lee*[a]

[a]*Department of Materials Science and Engineering, Yonsei University, 134 Shinchon, Seoul 120-749, Korea. E-mail: wooyoung@yonsei.ac.kr*

[b]*Department of Physics, Columbia University, New York, New York 10027, USA.*

1. Calibration of temperature difference for the Seebeck measurement

As described in the Measurement technique section, the temperature difference between two thermometers was obtained by calibrating the resistance difference of the thermometers. However, the absolute value of the temperature coefficient of resistance (TCR) was not used to calibrate the temperature. Practically, instead of the TCR, the change in the signal obtained using an AC lock-in amplifier was used, where the signals (V_{T1} and V_{T2}) were obtained at two different ambient temperatures (T_1 and T_2). The difference between the obtained signals ($\Delta V = V_{T1} - V_{T2}$) was converted to the temperature coefficient of signal (TCS, $\Delta V/\Delta T$) using the temperature difference ($\Delta T = T_1 - T_2$). Consequently, using the TCS, we can calibrate the signal obtained from the thermometers to the temperature. The actual calibration process was as follows.

(1) The change in the thermometer signals is obtained using a lock-in amplifier as a function of the heater voltage at two different ambient temperatures: for temperature calibration at 300 K, the two ambient temperature are 300 and 305 K [Figure S1(a)]. (2) The average signal difference between 300 and 305 K is calculated by subtraction and divided by the temperature difference, 5 K, to obtain the TCS at 300 K [Figure S1(b)]. (3) The signal obtained at 300 K is converted to the temperature using the TCS at 300 K [Figure S1(c)]. Using this process, we could obtain the

temperature change of the two thermometers as a function of the heater voltage, and using the difference between these temperature changes, we could obtain the temperature difference between the two thermometers.

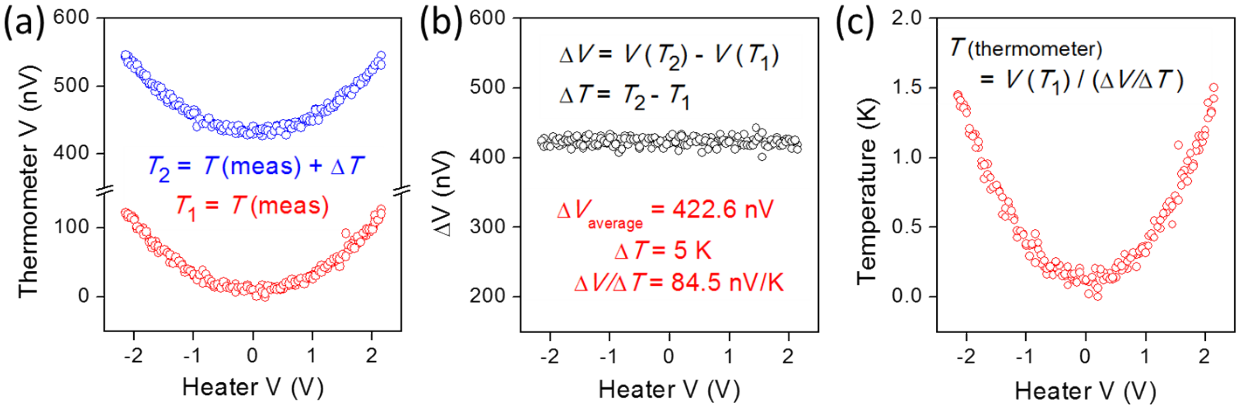

Figure S1 Signal process for temperature calibration; $T_1 = 300$ K and $T_2 = 305$ K.

2. Electrical resistivity of Bi nanowires for diameters in the 40–200 nm range

The resistivity trend could be divided into two diameter ranges up to 40 nm, as shown in Figure 2(b). Practically, in the large-diameter range (40–200 nm), the interpretation of the resistance in Bi nanowires is problematic because it is difficult to distinguish the changes in carrier density and mobility.[S1] In particular, the significant increase in the resistivity as the diameter decreases from 100 to 40 nm is difficult to explain solely by surface scattering. Although previous studies on the resistivity (resistance) of Bi nanowires interpreted their results as competition between the carrier density and mobility,[S1–S3] we added another mechanism, which is related to the carrier effective mass according to the theoretical[S4] and experimental[S5] studies reported.

In semimetallic Bi, the quantum confinement effect due to size reduction can easily occur owing to its unique intrinsic properties.[S6,S7] In typical metals and semiconductors, the size of 100 nm is too large to obtain quantum effects. In Bi nanowires, however, the band structure begins to change at a diameter of about 400 nm.[S4] This is caused by the extremely low carrier effective masses of Bi (the lowest value is $0.001m_0$). The band gap energy of subbands (L-point electron pockets and T-point hole pocket) is proportional to $\sqrt{\pi^2\hbar^2/m^* d^2}$. Therefore, the rate of band gap increase with decreasing diameter has a reciprocal relationship with the effective mass.[S6,S7] When the effective mass is constant and the diameter is 100 nm, the value of $\sqrt{\pi^2\hbar^2/m^*d^2}$ is calculated as 75 meV, which is larger than the band gap energy of the L-point subband (15 meV at 77 K and 36 meV at 300 K). According to a carefully calculated band-edge energies,[S4] however, the strong coupling between the valence and conduction bands of the L-point causes an increase in the effective mass with increasing band gap. As a result, the critical diameter of the semimetal-to-semiconductor (SMSC) transition decreases from 70 to 35 nm when the Lax two-band model, which includes the coupling effect, is used.[S4] The relationship between the effective mass, band gap energy, and coupling is given by[S8]

$$\frac{1}{m^*} = \frac{1}{m_0} + \frac{2}{{m_0}^2}\frac{|\langle v|p|c\rangle|^2}{E_g} - \frac{12\hbar^2k^2|\langle v|p|c\rangle|^4}{{E_g}^3{m_0}^2},$$

where $|\langle v|p|c\rangle|$ is the coupling term between the valence band v and conduction band c. The calculated band gap of the L-point subband at 100 nm is approximately twice that at 400 nm.[S4] As shown in Reference S4, the band gap of the L-point subband increases rapidly below about 100 nm; hence, the electron effective mass of Bi increases significantly in this diameter range according to the equation above. Furthermore, this increase in the electron effective mass was revealed experimentally in a previous study on Bi nanowires using SdH, which showed that the electron effective mass of a 100-nm-diameter nanowire was three times larger than that of bulk Bi.[S5] This effect will increase with decreasing diameter until band gap opening (after band gap opening, the carriers induced by surface states will be dominant).

Consequently, although the carrier mobility and density dependencies were found to be a major cause of the resistance behavior of Bi nanowires used in studies on the temperature-dependent resistance in previous reports,[S1–S3] intensive investigation of the diameter-dependent resistivity showed that the scattering effect is not sufficient to explain the significant variation in the resistivity. According to the theoretical and experimental results, the strong coupling effect in the L-point subband resulting in an increase in the electron effective mass could be an additional explanation of the resistivity behavior, because this effect increased rapidly with decreasing diameter: the origin of this coupling effect, subband energy shifting, resembles the diameter-dependent resistivity for diameters of 40–100 nm. Moreover, the diameter-dependent Seebeck coefficient could also be explained by this phenomenon according to equation (1) in the manuscript.

3. Electrical resistivity of Bi nanowires for diameters of 20–40 nm

Another main issue in the electrical resistivity behavior appeared in the diameter range $20 < d < 40$ nm. In this range, the transport properties were intensively investigated because of band gap opening due to the quantum size effect (QSE).[S2,S9] Although the estimated carrier density induced by surface states was only three times larger than the bulk carrier density ($n = \sim 3 \times 10^{18}$ cm^{-3}), this value was that of large-diameter nanowires ($d >> 100$ nm), which have bulk characteristics. In other words, the carrier-density-induced bulk-electronic band decreased with decreasing diameter owing to band shifting originating from QSE; hence, the carrier density of the 40-nm-diameter nanowire was significantly smaller than the carrier density induced by surface states, as shown in the band schematics in the Figure 2(d) insets. The fact that the resistivity values of 21 and 27 nm were comparable to the smallest resistivity values in the large diameter range could be attributed to the slight different between the carrier densities (only a factor of three). Briefly, although metallic surface states cause a significant decrease in the resistivity as the diameter decreases from 40 to 20 nm because of the reduced resistivity at 40 nm, the resistivity value at 20 nm can be comparable to the value for large-diameter nanowires [Figure 2(b)].

However, an unsolved problem remains: why did the surface states not dominate bulk transport at diameters larger than 40 nm? We thought that it can be attributed to the difference in the crystal orientation of the nanowires. Although the critical diameter of the SMSC transition (band gap opening) and the surface-state-dominant transport is known to be about 50 nm,[S2] it could vary with the crystal orientation of Bi.[S7] Practically, the critical diameter of a binary nanowire is smaller than that of a trigonal nanowire ($d_c = 50$ nm). In the binary Bi nanowires used in this study, the critical diameter was expected to be in the 20–40 nm range; hence, the maximum resistivity appeared at about 40 nm. In other words, with decreasing diameter, the band shifting due to QSE, which increases the resistivity, was dominated by the surface state effect, which decreases the resistivity, at a diameter of 40 nm.

Although we calculated the surface carrier density using the references in the manuscript, it was very challenging to obtain the absolute values of intrinsic properties such as the carrier density, effective mass, and mean free path~~,~~ as a function of the diameter in a nanowire structure. In nanowire studies, various techniques that are useful in studies of thin films and bulk cannot be adopted to characterize the properties owing to the spatial restriction of the one-dimensional structure. In practice, magneto-transport techniques including SdH oscillation were mainly employed in studies on nanowire structure to determine its intrinsic properties. In previous studies, we obtained the intrinsic properties of Bi nanowires using these indirect methods: an SdH study of 400-nm-diameter Bi nanowires revealed bulk-like characteristics,[S10] an SdH study of 100-nm-diameter Bi nanowires found an increase in the carrier effective mass and decrease in the carrier density due to QSE,[S5] and a quantum oscillation study of 30-nm-diameter Bi nanowires revealed two-dimensional transport characteristics due to surface states.[S11] From these previous studies, we obtained information on the intrinsic properties of Bi nanowires as functions of the diameter and interpreted the variation in the thermoelectric properties with diameter.

References

S1. J. Heremans, C. M. Thrush, Y. M. Lin, S. Cronin, Z. Zhang, M. S. Dresselhaus and J. F. Mansfield, Phys. Rev. B, 2000, 61, 2921-2930.

S2. T. E. Huber, A. Adeyeye, A. Nikolaeva, L. Konopko, R. C. Johnson and M. J. Graf, Phys. Rev. B, 2011, 83, 235414.

S3. T. E. Huber, A. Nikolaeva, D. Gitsu, L. Konopko, C. A. Foss and M. J. Graf, Appl. Phys. Lett., 2004, 84, 1326-1328.

S4. T. W. Cornelius and M. E. T. Molares, Nanowires, InTech, Shanghai, 2010.

S5. J. Kim, D. Kim, T. Chang and W. Lee, Appl. Phys. Lett., 2014, 105, 123107.

S6. M. S. Dresselhaus, G. Dresselhaus, X. Sun, Z. Zhang, S. B. Cronin and T. Koga, Phys. Solid. State, 1999, 41, 679-682.

S7. Y. M. Lin, X. Z. Sun and M. S. Dresselhaus, Phys. Rev. B, 2000, 62, 4610-4623.

S8. M. R. Black, Y. M. Lin, S. B. Cronin, O. Rabin and M. S. Dresselhaus, Phys. Rev. B, 2002, 65, 195417.

S9. P. Hofmann, Prog. Surf. Sci., 2006, 81, 191-245.

S10. W. Shim, J. Ham, J. Kim and W. Lee, Appl. Phys. Lett., 2009, 95, 232107.

S11. J. Kim, S. Lee, Y. M. Brovman, M. Kim, P. Kim and W. Lee, Appl. Phys. Lett., 2014, 104, 043105.